

## Hazard and Safety Regions for Paths with Constrained Curvature

Lei Shen, Vladimir J. Lumelsky\* and Andrei M. Shkel

*University of Wisconsin-Madison, Dept. of Mech. Engg., 1513 University Avenue, Madison,  
WI 53706, USA*

Communicated by B. Brosowski

In this paper the problem of collision analysis for a mobile robot operating in a planar environment with moving objects (obstacles) is addressed. The pattern of motion of the potential obstacles cannot be predicted; only a bound on their maximum velocity is available. Based on this information, at its current position the robot constructs the *Hazard Region* that corresponds to the path it contemplates. If the Hazard Region contains at least one obstacle, then there is a potential for this obstacle to collide with the robot (in which case perhaps another path should be planned). We first derive the solution for Hazard Region for two standard path primitives, a straight line segment and a circular arc segment; the solution is exact, except for one special case (for which the approximation error is estimated). This result is then applied to a more complex case when the path presents a combination of those primitives. Such are, for example, the optimal (shortest) paths with constrained curvature (known as Dubins paths [3]), which connect two points, each with a prescribed direction of motion. © 1998 B. G. Teubner Stuttgart—John Wiley & Sons, Ltd.

### 1. Introduction

We address one problem of motion planning and collision avoidance that appears in robotics. A point mobile robot  $R$  operates in a planar environment with moving objects (obstacles)  $O$  whose maximum possible velocity  $v_O$  is known but whose future trajectories are unpredictable. The robot can detect obstacles using its sensors. Starting at its current position  $S$ , the robot's goal is to reach, collision-free, some target point  $T$  along a specified path  $C$ . Based on  $C$  and  $v_O$ , the robot will attempt to construct the *Hazard Region* (HR). If any point of HR is occupied currently by an obstacle, the path is potentially unsafe. (In this latter case, perhaps another path should be contemplated and tested for HR). The complement of HR in the scene is called the *Safety Region* (SR).

Note that though under this approach the system would not need to check directly for potential collisions, it still needs to calculate distances between objects and the corresponding HR. The problem of detecting collisions between moving objects has been a popular topic in robotics literature (see, e.g., [4, 1, 2, 7, 10]). A variety of

\* Correspondence to: Vladimir J. Lumelsky, University of Wisconsin-Madison, Dept. of Mech. Engg., 1513 University Avenue, Madison, WI 53706, USA

approaches have been considered: checking for collision based on a finite number of motion sampling; collision analysis in space-time; representation of moving objects by their sweeping space–time volumes; calculation of collision point between two objects via a recursive division of space. A closely related problem is one of determining the minimum distance between two objects in two and three dimensions [6, 9].

A problem somewhat similar to ours, called the *pursuit-evasion problem*, is considered in differential games. Applications that motivate such work include, for example, decision-making in the interaction between a torpedo and a ship, or a missile and an aircraft, or two football players in the field. The assumption is that no information about the objects' trajectories is available, and so the worst case scenario is used. The problem is usually formulated as a minimax control problem for a system of differential equations describing the kinematics and dynamics of the controlled system. Typically, no analytic solutions are feasible; suggested heuristics are computationally intensive.

An alternative scenario that is more realistic for the robot collision avoidance problem is considered in this work. We assume that the trajectory of one party (the robot) is known whereas the other (the "pursuer") can move in the worst possible ways, subject to velocity constraints. In this scenario, at a given moment the robot contemplates a piece of the path and estimates its safety by calculating the surrounding Hazard Region (HR), which depends on the robot's path and velocity, and the known bound on the obstacles' maximum velocity. If the HR contains at least one obstacle, this means the path's safety cannot be guaranteed, in which case the robot would have to consider some other path.<sup>1</sup> Here a method is developed for fast computation of the Hazard Region for two standard path primitives, a straight-line segment and a circular arc segment, as well as any combination of those.

As the number of obstacles will not be important for our purpose, suppose there is only one obstacle in the scene,  $O$ . Robot  $R$ , currently at a starting point  $S$ , intends to move to the target point  $T$  – say, along a straight-line path. If  $R$  is close to  $T$  and  $O$  is sufficiently far away from  $R$  and  $T$ , the straight-line motion would be safe. Clearly, there is a set of points, a boundary curve, which separates safe initial positions of  $O$  from unsafe. Points on one side of this boundary represent the Hazard Region, and points on its other side—the complementary Safety Region.

There are two models of motion one can consider. Under the first model, also used in this work and referred to as *simple motion* in differential games theory and *holonomic motion* in mechanics and robotics, no restrictions are imposed on the geometry of robot paths. The second model restricts the paths to a bounded curvature (no sharp turns are allowed). That model, referred to as *nonholonomic motion*, is often more realistic in that it reflects constraints on motion due to the system kinematics (as in a car) or dynamics (such as the effect of masses and inertia).

Below, a method for HR calculation is first developed for the case when the robot and the obstacle are points. The method is then generalized to the case when both objects have dimensions, namely are circular bodies. Another case to consider will be

<sup>1</sup> A related question, not considered here, is one of existence of a path that would keep the robot outside the corresponding Hazard Region.

a situation when the robot starts its motion with some time delay relative to the obstacle’s motion. While algorithmically this case is shown to reduce to the case with circular objects, it becomes a tool for handling a more complex case where the robot’s contemplated path presents a combination of straight-line segments and circular arcs. The latter case appears, for example, in the optimal (shortest) paths with constrained curvature, known as Dubins paths [3]; each such path connects two points in the plane, each with a prescribed direction of motion.

After introducing the necessary notation and definitions in section 2, a case when the obstacle’s velocity is above that of the robot is considered in section 3, followed by the case when the obstacle’s velocity is below that of the robot. It turns out that in the latter case the straight-line motion and the circular motion need be treated somewhat differently; this is done in sections 4 and 5, respectively. In the case when the obstacle’s velocity is higher than that of the robot, a closed-form (exact) solution for the Hazard Region for both the straight-line and circular motion is obtained. For the case when the obstacle is slower than the robot, a closed-form solution for the straight-line motion and an approximate solution for the circular motion are obtained. The estimation error for the latter case is evaluated in section 6. Generalization to dimensioned (circular) objects and to the time delay in the robot’s starting moment is done in section 7. The case of complex multi-segment paths concludes the derivation of the proposed method, section 8. Some proofs, omitted for the lack of space, can be found in [8].

**2. Notation and definitions**

Given the maximum velocities of the robot  $R$  and obstacle  $O$ , denoted by  $v_R$  and  $v_O$ , respectively, and a robot’s path  $C$ , the goal is to find the corresponding Hazard Region, denoted HR (or equivalently, finding the Safety Region, denoted SR). Assume initially that  $R$  and  $O$  are points (the methodology will be later extended to circular objects, section 7).

A point  $O_0$  is said to *belong* to HR if and only if there exists a path for obstacle  $O$  starting at  $O_0$ , such that  $O$  would collide with  $R$  at some point of  $C$ . Without loss of generality, assume a unit robot velocity,  $v_R = 1$ , and  $v_O = v$ . We can do it because to decide whether a point is in the HR, it is enough to know the ratio  $v = v_O/v_R$ . Region HR is fully determined by the path  $C$  and value  $v$ ; write it as  $HR(C, v)$ , and similarly,  $SR(C, v)$  for the Safety Region. The formal definition then is

**Definition 1.** Let  $v > 0$  and  $a(t), b(t)$  be continuous functions of  $t$  on  $[0, t_T]$ . Then the Hazard Region for the path

$$C : \begin{cases} x = a(t), \\ y = b(t), \end{cases}$$

with the time delay  $\delta$  and  $0 \leq t \leq t_T$ , is defined as  $HR_\delta(C, v) = \{(x, y) | \exists t_M \in [0, t_T] \text{ s.t. } (x - a(t_M))^2 + (y - b(t_M))^2 \leq [v(t_M + \delta)]^2\}$ .

Time  $\delta$  is the robot  $R$ 's delay in starting the motion. Obstacle  $O$  is assumed to move without delay and in the worst possible way (i.e. doing its best in intercepting the robot);  $HR(C, v)$  will denote the situation without time delay. With this definition, note that if at any time during  $R$ 's motion obstacle  $O$  appears in its Safety Region  $SR$ , this means that by simply moving along the contemplated path robot  $R$  is guaranteed a collision-free passage to the target  $T$ .

We consider two classes of motion: (i) when the obstacle's maximum velocity is above that of the robot,  $v_O \geq v_R$ , i.e.  $v \geq 1$ , and (ii) when the opposite is true,  $v_O < v_R$ , i.e.  $v < 1$ . It is shown below that for the class (i) it is possible to obtain some general results on safety regions: however, for class (ii) the safety region depends on the specific form of the path curve  $C$ .

### 3. Motion with $v \geq 1$

Consider a case when  $v \geq 1$  and  $C(S, T)$  is a straight line segment. Suppose  $|C(S, T)| = d$  and  $v > 1$ . Then the robot  $R$ , starting at point  $S$  at time  $t_S = 0$ , will reach point  $T$  at time  $t_T = d$ . Choose a rectangular coordinate system  $(x, y)$ , with the origin at  $S(0, 0)$  and the positive direction of  $x$ -axis toward  $T(d, 0)$ . Suppose at moment  $t = 0$  obstacle  $O$  is at point  $P_0$ , Fig. 1. Consider a time moment  $t_M \in [0, t_T]$ . Since obstacle  $O$  can move in arbitrary directions with the maximum velocity  $v$ , within the time interval  $t_M$  it can cover distance  $v \cdot t_M$  from point  $P_0$ , and thus reach some points of segment  $(S, T)$ . Let us say, the farthest such point on  $(S, T)$  is point  $M$ , Fig. 1. Note that  $|P_0, M| > |S, M)$ . Therefore, there is a circle of radius  $v \cdot t_M$  centered at  $M$  (circle I, Fig. 1), such that if at moment  $t = 0$  obstacle  $O$  is within that circle, there is a potential for it to collide with robot  $R$  somewhere within the segment  $(S, M)$ . This means that point  $P_0$  belongs to the Hazard Region  $HR$  that corresponds to

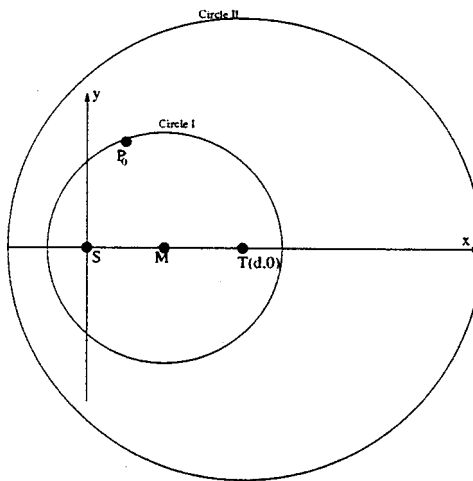


Fig. 1.  $HR(C, v)$  for a straight line path  $C(S, T)$  and  $v > 1$ .

a would-be robot's path  $C(S, M)$ . For any time moment  $t_{M_1} > t_M$ , a larger HR circle will appear. In general, if at moment  $t = 0$  the obstacle is anywhere within the disc of radius  $v \cdot t_d$  centered at  $T$ , it might collide with  $R$  at some point of segment  $(S, T)$ . Circle II in Fig. 1 thus presents the whole Hazard Region for the path  $C(S, T)$ .

Hence:

$$\begin{aligned}
 P_0(x_0, y_0) \in \text{HR}(C, v) \\
 \Leftrightarrow \min_{t_M \in [0, d]} [(t_M - x_0)^2 + y_0^2 - v^2 t_M^2] \leq 0 \\
 \Leftrightarrow |P_0 T| \leq vd
 \end{aligned}$$

**Proposition 1.** *If  $C$  is a straight-line segment connecting  $S$  and  $T$ , with  $|ST| = d$ , then  $\text{HR}(C, v) = \{O_0 : |O_0 T| \leq vd\}$ , where  $O_0$  refers to possible starting positions of obstacle  $O$ .*

The statement simply states that if and only if  $O$  can reach  $T$  before  $R$  does,  $R$  could be “captured”. This is obvious: if  $O$  can collide with  $R$  at any point on path  $C$ , then it will be able to reach  $T$  before  $R$  does it, because  $v \geq 1$  (i.e.  $v_O \geq v_R$ ). This is stated as:

**Proposition 2.** *If  $v \geq 1$  and  $|C| = d$ , then  $\text{HR}(C, v) = \{P_0 : |P_0 T| \leq vd\}$ .*

One can draw a similar argument for any point of the path  $C(S, T)$ . Consider an arbitrary point  $M$  on path  $C$ , Fig. 1. If the part of  $C$  from  $S$  to  $M$  is of length  $d_M$ , then it takes time  $t = d_M$  for robot  $R$  to reach  $M$ . By this time the maximum distance that obstacle  $O$  could possibly travel is  $vd_M$ . Hence to make certain that  $O$  will not be able to capture  $R$  at point  $M$ ,  $O$  has to be initially located beyond the distance  $vd_M$  from  $M$ . For this to happen, the initial location of  $O$  has to be outside the disc of radius  $vd_M$  centered at  $M$ . A similar disc, called the *Hazard Disc*,  $\text{HD}(C, v, M)$ , will appear for any other point  $M$  on  $C$ .

**Proposition 3.**  $\text{HR}(C, v) = \bigcup_{M \in C} \text{HD}(C, v, M)$ .

The fact that HR is the union of all the HDs is important and will be used later. Clearly, the disc  $\text{HD}(C, v, T)$  is always the biggest among all HDs. To summarize, for the case when  $v \geq 1$ , the Hazard Region contains all the HDs,  $\text{HR}(C, v) = \text{HD}(C, v, T)$ .

#### 4. Straight-line Motion with $v < 1$

For the case  $v \geq 1$  it was shown above that the length of path  $C$  is sufficient to find  $\text{HR}(C, v)$ . The case  $v < 1$  is more complicated: the Hazard Region analysis depends on the curve along which the robot travels. Consider first the straight-line motion, and then a circular motion.

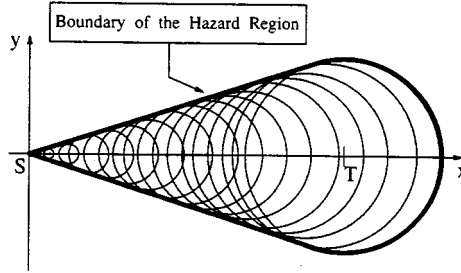


Fig. 2. The Hazard Region  $HR(C, v)$  for the straight-line path segment  $C(S, T)$  and parameter  $v < 1$ . The region is a union of growing circles.

To find the starting positions  $O_0$  of the obstacle that belong to the Hazard Region, proceed as follows (see Fig. 2). (Given our assumption that the robot velocity is 1, the time  $t_M$  in expressions like  $(t_M - x_0)$  is also used below as a length quantity.)

$$\begin{aligned}
 &O_0(x_0, y_0) \in HR(C, v) \\
 &\Leftrightarrow \min_{t_M \in [0, d]} [f_1(t_M) = (t_M - x_0)^2 - v^2 t_M^2 + y_0^2] \leq 0 \\
 &\Leftrightarrow (\text{since } v < 1) \\
 &\quad \begin{cases} f_1(t_{\min}) \leq 0 & (t_{\min} = \frac{x_0}{1-v^2} \in [0, d]) \\ f_1(0) \leq 0 \text{ or } f_1(d) \leq 0 & (t_{\min} = \frac{x_0}{1-v^2} \in [0, d]) \end{cases} \\
 &\Leftrightarrow \begin{cases} \frac{-v_0}{1-v^2} x_0^2 + y_0^2 \leq 0 & (x_0 \in [0, (1-v^2)d]) \\ (x_0, y_0) = (0, 0) \text{ or } (x_0 - d)^2 + y_0^2 \leq v^2 d^2 & (\text{else}) \end{cases} \\
 &\Leftrightarrow |y_0| \leq \frac{v}{u} |x_0| \text{ (if } x_0 \in [0, u^2 d]) \text{ or } (x_0 - d)^2 + y_0^2 \leq v^2 d^2,
 \end{aligned}$$

where  $u = \sqrt{1 - v^2}$ . This leads to

**Proposition 4.** *If  $v < 1$  and path  $C(S, T)$  is a straight-line segment, then*

$$HR(C, v) = \{P_0(x_0, y_0) : |y_0| \leq \frac{v}{u} |x_0| \text{ (} x_0 \leq u^2 d \text{) or } (x_0 - d)^2 + y_0^2 \leq v^2 d^2\} \text{ where } u = \sqrt{1 - v^2}.$$

Figure 2 illustrates the Hazard Region  $HR$  for  $v = 0.33$ . Also shown is a union of growing discs  $HD$  with centers on the path  $C(S, T)$ . The final  $HR$  is an inside of the cone limited by lines  $|y| = v/u|x|$  tangent to the disc  $HD(C, v, T)$ ; the latter closes the Hazard Region.

### 5. Circular motion with $v < 1$

Turning now to the case of a circular arc path  $C$ , set the origin  $O$  of a rectangular co-ordinate system  $(x, y)$  at the centre of the circle;  $OS$  is the positive direction of

$x$ -axis. Without loss of generality, assume that the radius of the circle is 1. Let  $C$  be an arc of  $\omega$  radians,  $0 \leq \omega \leq 2\pi$ . The Cartesian co-ordinates of points  $S$  and  $T$  are thus  $(1, 0)$  and  $(\cos \omega, \sin \omega)$ , respectively. Robot  $R$  moves along  $C$  counter-clockwise.

Given the circular path  $C$ , it is convenient to use here a polar coordinate system,  $(\rho, \theta)$ , with the same origin  $O$  and the  $x$ -axis as in the chosen rectangular system. The polar coordinates for  $S$  and  $T$  are  $(1, 0)$  and  $(1, \omega)$ . HR can now be found similar to the straight line case, as follows.

Since it takes robot  $R$  time  $t_M$  to reach point  $M(1, t_M)$ , all the points in the plane that are at distance no more than  $vt_M$  from  $M$  belong to HR. Consider any point  $P_0(\rho_0, \theta_0)$  in the plane. In the triangle  $OP_0M$ , the distance from  $P_0$  to  $M$  is given by

$$|P_0M| = \sqrt{1^2 + \rho_0^2 - 2\rho_0 \cos(\theta_0 - t_M)}. \tag{1}$$

Therefore,

$$\begin{aligned} P_0(\rho_0, \theta_0) \in \text{HR}(C, v) & \\ \Leftrightarrow \exists t_M \in [0, \omega] \text{ such that } |MP_0| \leq vt_M & \\ \Leftrightarrow \exists t_M \in [0, \omega] \ 1^2 + \rho_0^2 - 2\rho_0 \cos(\theta_0 - t_M) \leq v^2 t_M^2 & \\ \Leftrightarrow \min_{t_M \in [0, \omega]} [1 + \rho_0^2 - 2\rho_0 \cos(\theta_0 - t_M) - v^2 t_M^2] \leq 0. & \end{aligned}$$

The critical point(s) of

$$f_2(t_M) = 1 + \rho_0^2 - 2\rho_0 \cos(\theta_0 - t_M) - v^2 t_M^2 \tag{2}$$

are the roots of the equation

$$\sin(\theta_0 - t_M) + \frac{v^2}{\rho_0} t_M = 0 \tag{3}$$

which is transcendental and may have zero, one, two, or three solutions depending on the values  $\rho_0, \theta_0, \omega$  and  $v$ , see Fig. 3. Although it can be shown that at most one of its roots corresponds to a minimum of  $f_2(t_M)$ , ours not being able to find its value analytically makes it difficult to find the boundary curves of HR from this analytical approach.<sup>2</sup>

Figure 4 shows examples (obtained with the MATLAB package) of the Hazard Region for circular motion, with different values of  $\omega$  and  $v$ . [Note that alternatively, given point  $P_0(\rho_0, \theta_0)$ , one could find  $\min_{t_M \in [0, \omega]} f_2(t_M)$ , and hence determine whether  $P_0$  belongs to the HR.] The same values of  $v$  and  $\omega$  will also be used later to compare these results with other approximations.

For the sake of computational savings and for further insight, we now attempt to find an approximation of the HR for circular motion, in a simple and explicit form.

<sup>2</sup> It has been suggested that these curves possibly can be found based on knowledge of cyclographic image of curves. This still remains an open question.

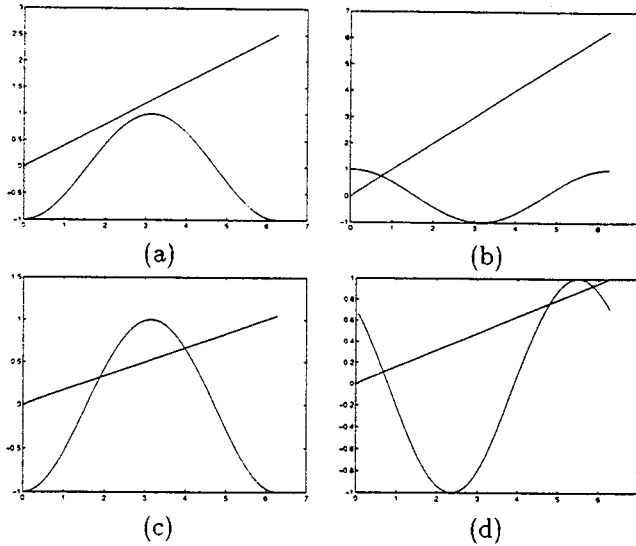


Fig. 3. Various cases of the number of roots in equation (3),  $\omega = 2\pi$ : (a) Zero roots:  $\theta = \pi/2, v = 0.2, \rho = 0.1$ ; (b) One root:  $\theta = 3\pi/2, v = 0.5, \rho = 0.25$ ; (c) Two roots:  $\theta = \pi/2, v = 0.67, \rho = 2.67$ ; (d) Three roots:  $\theta = 5\pi/4, v = 0.16, \rho = 0.16$ .

While planning the motion, robot  $R$  will need to know if obstacle  $O$  is currently within the Hazard Region of some desired path, and take further action accordingly. Therefore, to guarantee  $R$ 's safety, approximations of HR should be supersets of HR. The goal now is to find a set that contains the real HR, is a good approximation for most values of  $v$  and  $\omega$ , and is easy to compute.

First, consider the case when  $v \geq 1$ ; recall that the HR in this case is always a disc centered at  $T$ . Suppose the radius of this disc is  $D$ . By Proposition 3, this disc contains all the hazard discs HD. The best approximation of HR is given by

**Proposition 5.** *In the approximation problem above, let*

$$D = \begin{cases} 2 \sin \frac{\omega}{2} & (\text{if } \omega < 2 \cos^{-1} v), \\ 2u + v(\omega - 2 \cos^{-1} v) & (\text{if } \omega \geq 2 \cos^{-1} v). \end{cases}$$

*A disc centered at  $T$  contains all the HDs if and only if its radius is not less than  $D$ .*

The proof of this statement makes use of the following lemma.

**Lemma 1.**  *$v \in (0, 1)$ . Suppose  $0 < \omega \leq 2 \cos^{-1} v$ . Then  $2 \sin \omega/2 \geq v\omega$ .*

For the proofs of Proposition 5 and Lemma 1 refer to [8].



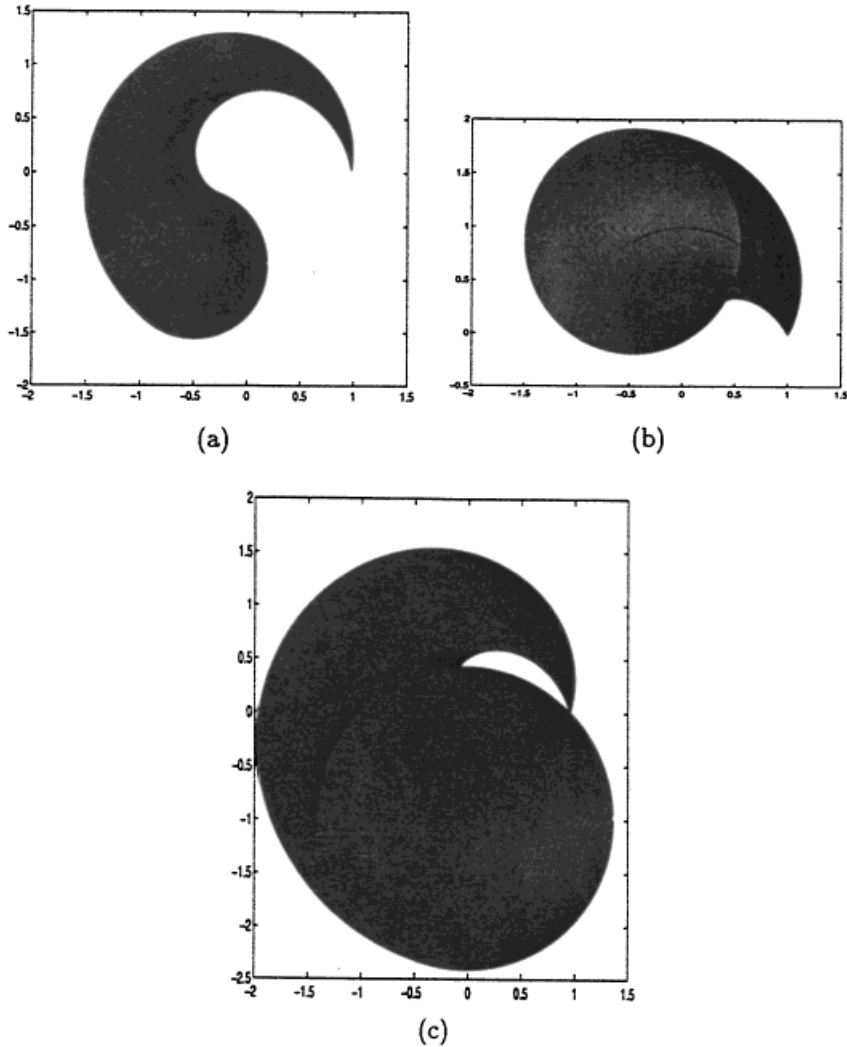


Fig. 4. HR for circular motion, with different values of  $v$  and  $\omega$ : (a)  $\omega = 4\pi/3$ ,  $v = 0.17$ ; (b)  $\omega = 2\pi/3$ ,  $v = 0.5$ ; (c)  $\omega = 3\pi/2$ ,  $v = 0.3$ .

With an approximate solution at hand, the next question is the approximation error. Some precise results on this appear in Section 6. Just to see how applicable our solution is, inspect briefly two cases, the relative error as  $v \rightarrow 0$ , and as  $v \rightarrow 1$ .

As shown above, if  $v \rightarrow 1$ , the difference between the entire HR and the final HD becomes smaller and smaller; when  $v = 1$  they become identical. Since solution obtained is the smallest disc centered at  $T$  and containing HR, as  $v \rightarrow 1$ , HR will approach the final HD as well. Hence, as  $v \rightarrow 1$ , the absolute error is approaching zero. But, the area of the real HR is approaching the area of the final HD for  $v = 1$ ,

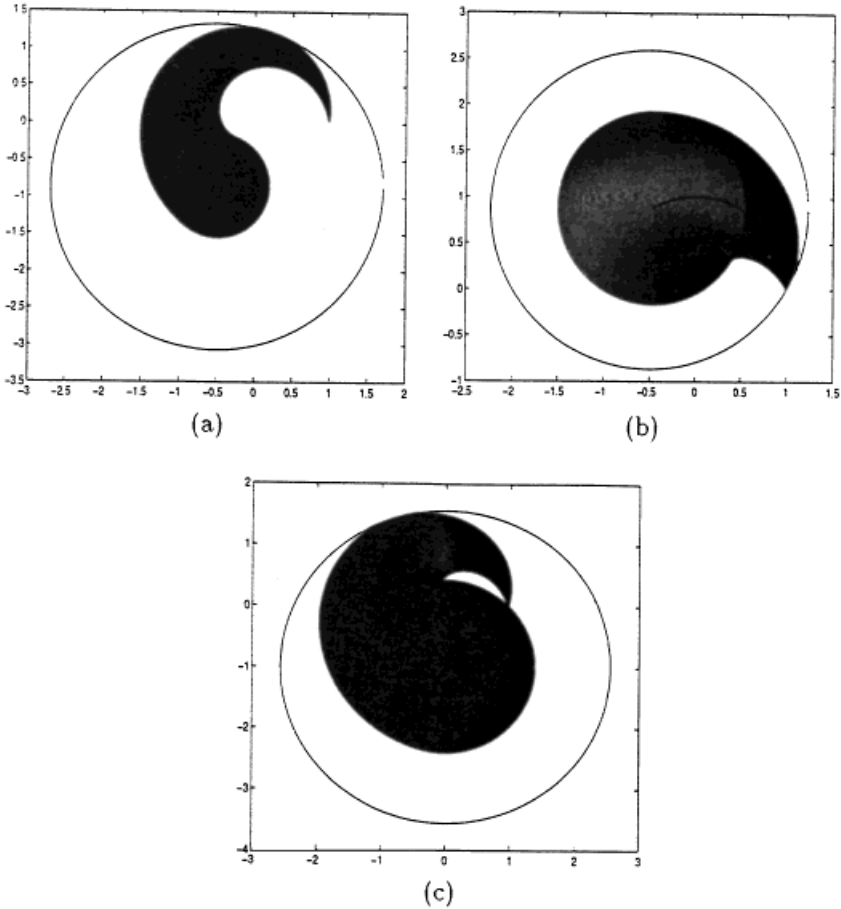


Fig. 5. Using one single disc centered at  $T$  to approximate the HR. The same  $v$  and  $\omega$  as in Fig. 4(a)–(c).

which is fixed. The conclusion therefore is that the relative error goes to zero – which suggests that the approximation obtained is particularly good when  $v$  is close to 1 (see Fig. 6(a)).

On the other hand, as  $v \rightarrow 0$ , apparently the area of the entire HR approaches zero. What happens to the solution then? Since it always contains HR, and since the starting point  $S$  always belong to HR (just like any other point on the path), the radius  $D$  of our solution disc is at least the distance between  $S$  and  $T$ , a constant.

The unfortunate conclusion here is that as  $v \rightarrow 0$ , the relative error goes to  $\infty$ . Shown in Fig. 6 are the approximations for  $\omega = \pi$  and several different values of  $v$ ; the error, which is the area between the circle (approximation) and the real HR is especially big for small  $v$ , Fig. 6(c).

It is therefore necessary to find another approximation for HR, one that works better for small values  $v$ . By combining it with the approximation above, a good

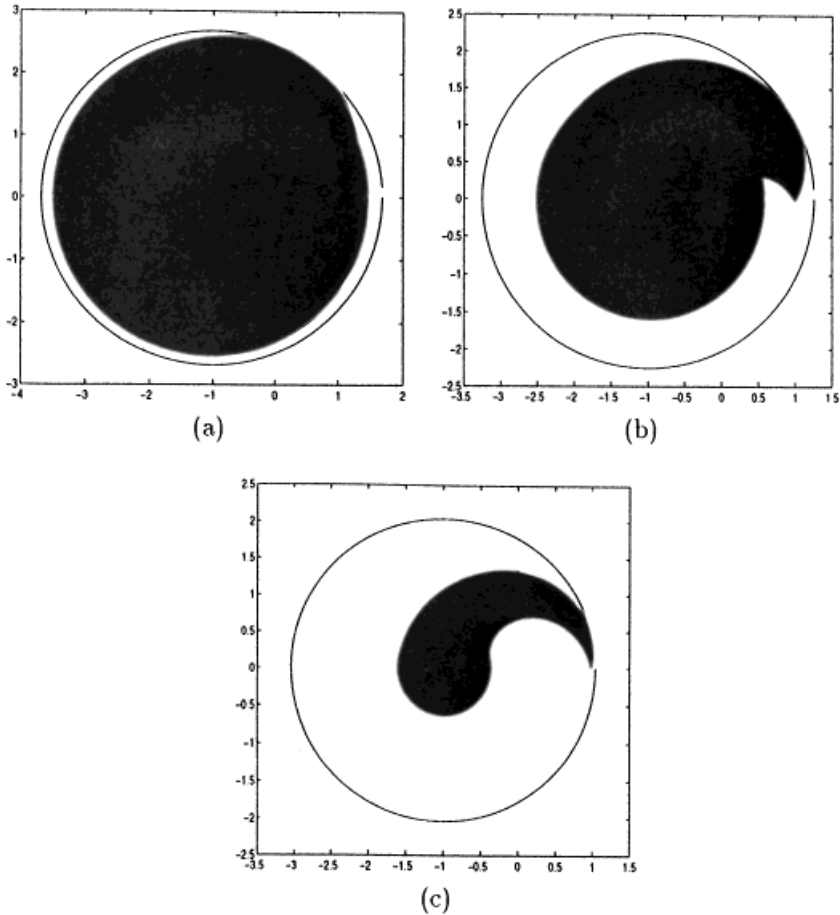


Fig. 6. The error of the first approximation for different velocities  $v$  ( $\omega = \pi$ ): (a) Small error,  $v = 0.8$ . (b) Average error,  $v = 0.5$ . (c) Big error,  $v = 0.2$ .

solution for any  $v \in (0, 1)$  is obtained. To find this new approximation, one cannot use a single disc to cover the HR; instead, a union of discs is used. Recall that any point  $M$  on path  $C$  has an associated hazard disc HD; the biggest of those, of radius  $v\omega$ , is the final disc. The union of all HDs is the exact solution. As those HDs are hard to work with, every HD is replaced by the biggest disc, the final HD.

The result is the second approximation solution, which presents a union of discs of the same radius  $v\omega$ , centered at points with polar coordinates  $(1, t_M)$ . Figure 7 provides two examples of this second solution, for  $v\omega < 1$  and  $v\omega > 1$ , respectively. To present this superset of HR explicitly, note that its points between lines  $\theta = 0$  and  $\theta = \omega$  constitute the set

$$\{P_0(\rho_0, \theta_0) \mid \rho_0 \in [1 - v\omega, 1 + \omega] \text{ and } \theta_0 \in [0, \omega]\}. \tag{4}$$

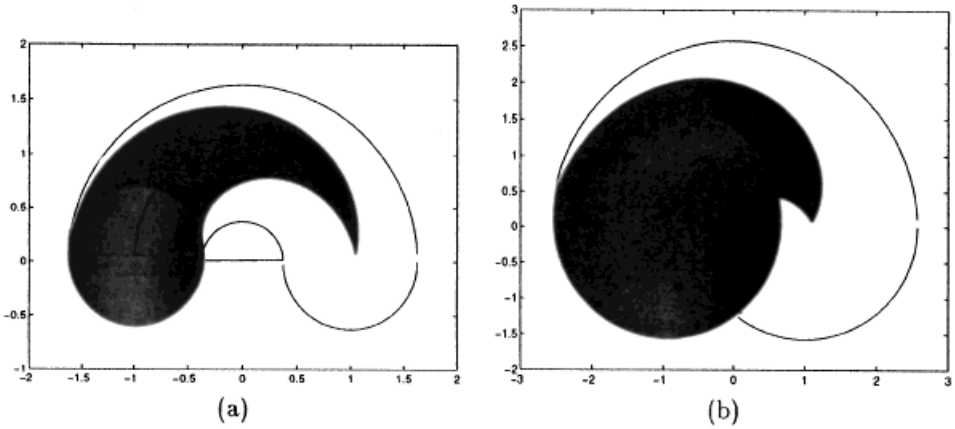


Fig. 7. Examples of the second approximation method: (a)  $\omega = \pi, v = 0.2$ ; (b)  $\omega = \pi, v = 0.5$ .

To include the half of disc  $HD(C, v, T)$  cut by the line  $\theta = \omega$ , and the similar half of the disc centered at  $S$  cut by  $\theta = 0$ , add the two discs,

$$\{P_0 \mid |P_0T| \leq v\omega \text{ or } |P_0S| \leq v\omega\}. \tag{5}$$

**Proposition 6.** *In the approximation problem above, the set  $\{P_0(\rho_0, \theta_0) \mid |P_0T| \leq v\omega \text{ or } |P_0S| \leq v\omega \text{ or } |P_0O| \in [1 - v\omega, 1 + \omega] \ \& \ \theta_0 \in [0, \omega]\}$  is a superset of  $HR(C, v)$ .*

Examples in Fig. 8 show how the superset just found approximates the exact solution.

**Remarks.** This idea can be explored further, leading to better approximations. Take a partition of  $[0, \omega]$ :

$$0 = \tau^0 < \tau^1 < \tau^2 < \dots < \tau^{n-1} < \tau^n = \omega. \tag{6}$$

Replace the HD for  $t_M$  by the HD at  $\tau^k$  provided that  $t_M \in (\tau^{k-1}, \tau^k]$ . Then the approximation will look as in the example in Fig. 9. This extension provides more accuracy at the price of more computational cost. If the computational savings cost is of minor concern, with a sufficiently small-normed partition of  $[0, \omega]$  any degree of accuracy can be achieved by this method.

### 6. Error estimation

Since the approximate solutions obtained above are supersets of the Hazard Region  $HR$ , the absolute approximation error is the difference between the area obtained and the area of the exact  $HR$ . As the latter is not available, an upper bound for the error

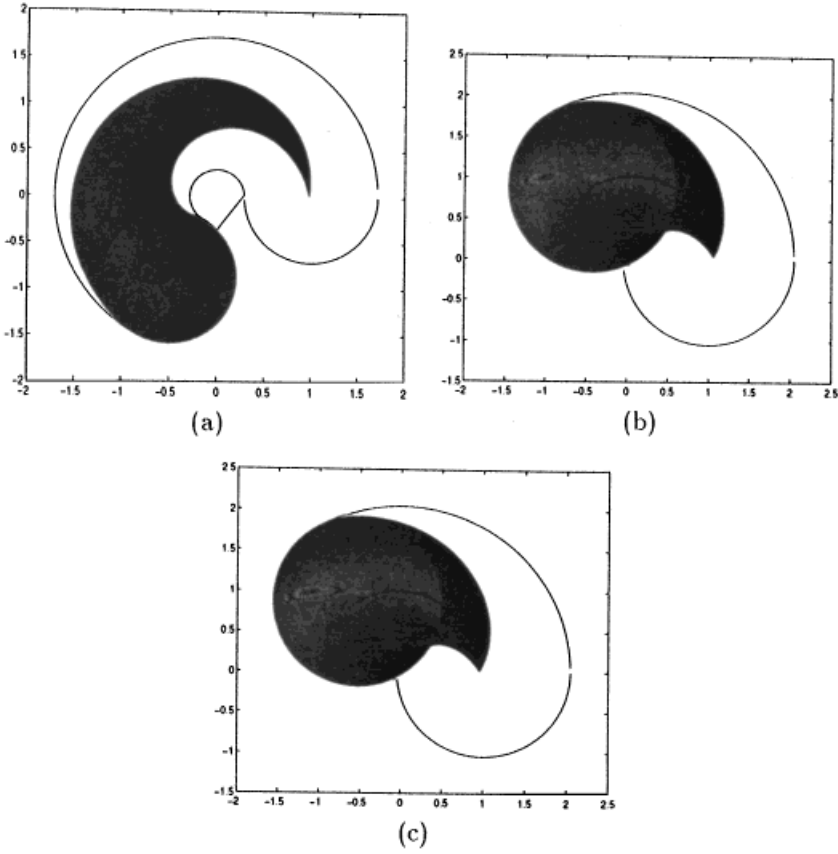


Fig. 8. Using a union of discs to approximate the HR. Here  $v$  and  $\omega$  are the same as in Fig. 4(a)–(c).

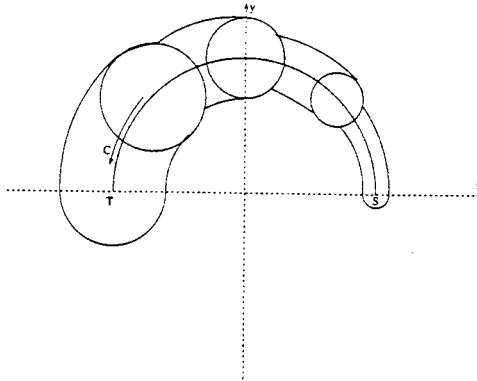


Fig. 9. A more accurate approximation is obtained by exploring the idea in the Remark.

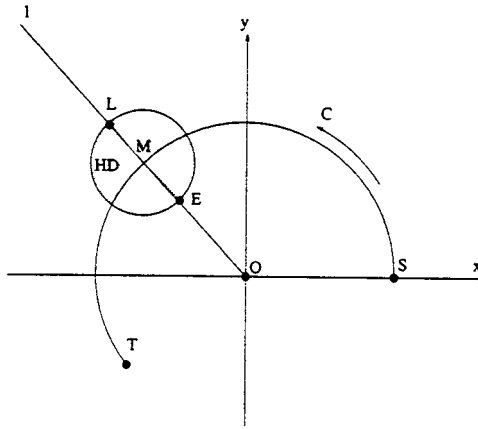


Fig. 10. The line  $l: \theta = \theta_0$  enters the HD at point  $E$  and leaves it at point  $L$ .

can be obtained by combining a lower bound on actual HR with an upper bound on the approximated HR. Start with the former: with the half of the final HD, i.e.

$$\{P(\rho, \theta) \mid d(P, T) \leq v\omega \text{ and } \theta \geq \omega\} \tag{7}$$

excluded, the remaining part of the actual HR lies between the lines  $\theta = 0$  and  $\theta = \omega$ . The half line  $\theta = \theta_0$  emanating from  $S$  for any  $\theta_0 \in [0, \omega]$  will enter the HR and eventually leave it. If  $v\omega \leq 1$ , then, as seen in Fig. 4(a),  $S$  is not included in  $HD(C, v, T)$  (because its radius is  $v\omega$ ). Hence, any half line similar to the above will enter and leave the HR only once, at points  $E(\rho_E, \theta_0)$  and  $L(\rho_L, \theta_0)$ , respectively.

The disc HD at  $M(1, \theta_0)$ , of radius  $v\theta_0$ , is contained in the HR; the half line  $\theta = \theta_0$  enters it at point  $(1 - v\theta, \theta_0)$  and leaves at  $(1 + v\theta, \theta_0)$  (see Fig. 10). Hence,<sup>3</sup>

$$\rho_E \leq 1 - v\theta_0, \quad \rho_L \geq 1 + v\theta_0 \tag{8}$$

and the region bounded by curves  $\rho = 1 - v\theta$ ,  $\rho = 1 + v\theta$ , and  $\theta = \omega$  is a subset of HR. Its area is given by

$$I = \int_0^\omega \int_{1-v\theta}^{1+v\theta} r \, dr \, d\theta = \int_0^\omega \frac{1}{2} r^2 \Big|_{1-v\theta}^{1+v\theta} d\theta = \int_0^\omega 2v\theta_0 \, d\theta = v\omega^2. \tag{9}$$

Then, the first lower bound for the area of HR is:

**Proposition 7.** *Let  $C$  be an arc of radius 1 and length  $\omega \in (0, 2\pi)$  radians, and  $v \in (0, 1)$ . If  $v\omega \leq 1$  then*

$$\text{Area}(HR(C, v)) \geq v\omega^2. \tag{10}$$

Moreover, if the part of HR between the lines  $\theta = 0$  and  $\theta = \omega$ , which was considered earlier, does not intersect the half of disc  $HD(C, v, T)$  that has excluded, the lower

<sup>3</sup> This can also be seen from the fact that  $\cos \beta \leq 1$  in the description of the exact HR given by (2).

bound can be further improved, to  $I + \frac{1}{2}\pi(v\omega)^2$ . It is not clear, however, under what conditions the said areas intersect. As discussed below, the important case is when  $\omega \leq 3\pi/2$ . In fact, our temporary assumption  $v\omega \leq 1$  is sufficient to obtain the next result:

**Proposition 8.** *Under the assumptions of the last proposition, if in addition it is known that  $\omega \leq 3\pi/2$ , then*

$$\text{Area}(\text{HR}(C, v)) \geq v\omega^2 + \frac{\pi}{2} v^2\omega^2. \tag{11}$$

This appears as follows. The half of disc  $\text{HD}(C, v, T)$  between lines  $\theta = \omega$  and  $\theta = \omega + \pi/2$  can intersect the portion of HR considered above only if it intersects the part between  $\theta = \omega - \pi$  and  $\theta = \omega - \pi/2$  (note that  $\omega + \pi/2 \leq 2\pi$ .) But this can happen only when that part extends over the origin  $O$ , to contain points with negative  $\rho$ -coordinate. This is impossible since  $v\omega \leq 1$ , hence no HD contains  $O$ .

The case  $v\omega \geq 1$  is more complicated, Fig. 4(c). Here,  $\rho = 1 + v\theta$  can be used as the outer boundary of the estimation, just like in the previous case. For the inner boundary, use  $\rho = 1 - v\theta$  where  $v\theta \leq 1$ , and use  $\rho = 0$  for the part where  $v\theta > 1$ . This corresponds to the region bounded by the curves  $\rho = 1 + v\theta$ ,  $\rho = 1 - v\theta$  ( $\theta = 1/v$ ), and  $\theta = \omega$ . Its area is

$$\begin{aligned} J &= \int_{1-v\theta}^{1/v} r \, dr \, d\theta + \int_{1/v}^{\omega} \int_0^{1+v\theta} r \, dr \, d\theta \\ &= v \left(\frac{1}{v}\right)^2 + \int_{1/v}^{\omega} \frac{1}{2} (1 + v\theta)^2 \, d\theta = \frac{1}{v} + \frac{1}{6v} (1 + v\theta)^3 \Big|_{1/v}^{\omega} = \frac{1}{6v} (1 + v\omega)^3 - \frac{1}{3v}. \end{aligned} \tag{12}$$

**Proposition 9.** *Let  $C$  be an arc of radius 1 and of length  $\omega \in (0, 2\pi)$  radians. If  $v \in (0, 1)$  and  $v\omega > 1$  then*

$$\text{Area}(\text{HR}(C, v)) \geq \frac{1}{6v} (1 + v\omega)^3 - \frac{1}{3v}. \tag{13}$$

Using the assumption  $\omega \leq 3\pi/2$ , this lower bound can be further improved. For  $v\omega > 1$ , one part of the final disc between  $\theta = \omega$  and  $\theta = 2\pi$  is still not included in the portion considered above, because the inner boundary has been taken as  $\rho = 0$  for  $\theta > 1/v$ . This means that no portion of the disc extends beyond the origin. To decide if the area of this part of  $\text{HD}(C, v, T)$  can be added to the previous estimation, one needs to know what fraction of the whole final HD it is. To find the latter, observe that if  $\omega \leq \pi$ , as in the case  $v\omega > \pi$ , then the half of  $\text{HD}(C, v, T)$  is completely between  $\theta = \omega$  and  $\theta = 2\pi$ . If  $\omega < \pi$ , [...] find the angle  $\alpha$  from the triangle  $TOI$ , Fig. 11. The result is

$$\alpha = \omega + \sin^{-1} \left( \frac{\sin \omega}{v\omega} \right). \tag{14}$$

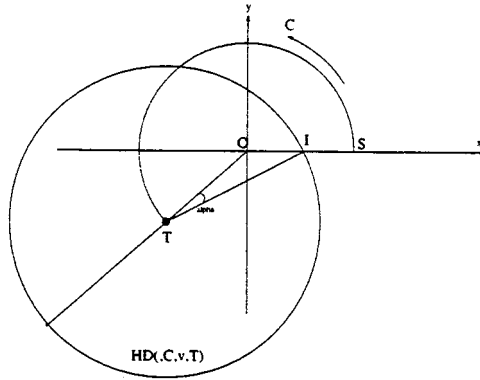


Fig. 11. Solve for angle  $\alpha$  to find the radian of the sector.

Recall that the fraction  $a = (\pi - \alpha)/2\pi$  of disc  $HD(C, v, T)$  has not been counted in the previous estimation. Therefore,

**Proposition 10.** Under the same assumptions on  $C, \omega$ , and  $v$  of the last proposition, if in addition  $\omega \leq 3\pi/2$  then

$$\text{Area}(\text{HR}(C, v)) \leq \begin{cases} \frac{1}{6v}(1 + v\omega)^3 - \frac{1}{3v} + \frac{\pi}{2}v^2\omega^2 & (\text{if } \omega \leq \pi), \\ \frac{1}{6v}(1 + v\omega)^3 - \frac{1}{3v} + a\pi v^2\omega^2 & (\text{if } \omega > \pi), \end{cases}$$

where

$$a = 1 + \frac{\omega - \sin^{-1}((\sin \omega)/v\omega)}{2\pi}.$$

When  $v$  is large, the final HD is almost the entire HR; the following fact is helpful:

**Proposition 11.**  $\text{Area}(\text{HR}(C, v)) \geq \pi(v\omega)^2$  which is the area of the HD above.

Turning now to the upper bounds for our approximate solution, obtain first a very simple solution for the HR area:

**Proposition 12.** The area of the first approximate solution is

$$S_1 = \pi D^2 = \begin{cases} \pi(\sin \omega/2)^2 & (\text{if } \omega < 2\cos^{-1} v), \\ \pi(2u + v(\omega - 2\cos^{-1} v))^2 & (\text{else}). \end{cases} \tag{15}$$

For the case  $v\omega < 1$ , the second solution is a part of a ring whose inner radius is  $(1 - v\omega)$  and outer radius is  $(1 + v\omega)$ . The result is,



**Proposition 13.** For  $v\omega < 1$ , the solution given in Proposition 6 becomes  $S_2 = 2v\omega^2 + \pi(v\omega)^2$ .

If  $v\omega > 1$ , the solution’s geometric shape is more complicated (see Fig. 7(b)). It can be, however, approximated, as follows. Find the area of the two sectors between  $\theta = 0$  and  $\theta = \omega$ , which are, respectively,

$$A_1 = \frac{\omega}{2\pi} (\pi(1 + v\omega)^2) = \frac{\omega(1 + v\omega)^2}{2}, \tag{16}$$

$$A_2 = \frac{\omega}{2\pi} (\pi(1 - v\omega)^2) = \frac{\omega(1 - v\omega)^2}{2}. \tag{17}$$

The areas of two halves of the discs at  $T$  and  $S$ ,

$$\begin{aligned} &\{P(\rho, \theta) \mid |PS| \leq v\omega \text{ and } \theta \leq 0\}, \\ &\{P(\rho, \theta) \mid |PT| \leq v\omega \text{ and } \theta \geq \omega\} \end{aligned} \tag{18}$$

add up to  $A_3 = \pi(v\omega)^2$ . The part of  $A_3$ , along with the first sector above, covers the entire approximate solution, with an overlapping part which contains the second sector. Therefore,

$$A = A_1 + A_3 - A_2 \tag{19}$$

is an upper bound of the area of the solution. Note that some area here has been counted more than once, see Fig. 7(b). Hence the estimate,

**Proposition 14.** If  $v\omega > 1$ , then the area of the set given in Proposition 6 is bounded from above by

$$S_2 = 2v\omega^2 + \pi v^2\omega^2. \tag{20}$$

Recall that our reason for attempting the second solution is to find a better approximation for small values of  $v$ . Has this goal been achieved? From Propositions 13 and 14, the absolute error of approximation is bounded by

$$(2v\omega^2 + \pi v^2\omega^2) - \left(v\omega^2 + \frac{\pi}{2} v^2\omega^2\right) = \left(v\omega^2 + \frac{\pi}{2} v^2\omega^2\right). \tag{21}$$

The relative error is thus less than 100%. That 100% turns out to be the answer is not surprising because the limiting case is analogous to approximating a triangle by a rectangle, as illustrated in Fig. 12. Since the area of the actual HR goes to zero, the relative error being less than 100% is a useful result. A better result for the case  $v \rightarrow 0$  can be obtained at the cost of more computation time, by making use of the remark following Proposition 6.

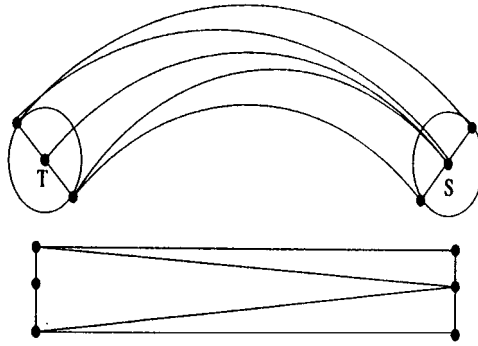


Fig. 12. The limiting case as  $v \rightarrow 0$ .

With two supersets of the HR now at hand, taking their intersection produces a better result than either of them. This intersection produced thus becomes our final solution (Fig. 13). To gain more insight in the magnitude of the approximation errors, consider now several examples. Let  $\omega = \pi$ , and consider three different values for  $v$ .

*Example 1.*  $v = \sqrt{3}/2 \approx 0.87$ .

By Proposition 11, Area of HR  $> \pi v^2 \omega^2 \approx 23.25$ .

By Proposition 12, Area of the first approximation  $< \pi(2u + v(\omega - 2\cos^{-1} v))^2 \approx 24.87$ .

By Proposition 14, Area of the second approximation  $< 2v\omega^2 + \pi v^2 \omega^2 \approx 40.35$ .

The relative error in the first approximation  $< 7.0\%$ .

The relative error in the second approximation  $< 73.5\%$ .

*Example 2.*  $v = 0.5$

By Proposition 10, Area of HR  $> \frac{1}{6v}(1 + v\omega)^3 - \frac{1}{3v} + \frac{\pi}{2}v^2\omega^2 \approx 8.87$ .

By Proposition 12, Area of the first approximation  $< \pi(2u + v(\omega - 2\cos^{-1} v))^2 \approx 15.98$ .

By Proposition 14, Area of the second approximation  $< 2v\omega^2 + \pi v^2 \omega^2 \approx 17.62$ .

The relative error in the first approximation  $< 80\%$ .

The relative error in the second approximation  $< 99\%$ .

*Example 3.*  $v = 0.2$

By Proposition 8, Area of HR  $> v\omega^2 + \frac{\pi}{2}v^2\omega^2 \approx 2.59$ .

By Proposition 12, Area of the first approximation  $< \pi(2u + v(\omega - 2\cos^{-1} v))^2 \approx 13.07$ .

By Proposition 14, Area of the second approximation  $< 2v\omega^2 + \pi v^2 \omega^2 \approx 5.18$ .

The relative error in the first approximation  $< 405\%$ .

The relative error in the second approximation  $< 100\%$ .

Note that different propositions are used for different values of  $v$ . It is easy to write a computer program to decide which version gives the best result, and then compute it.

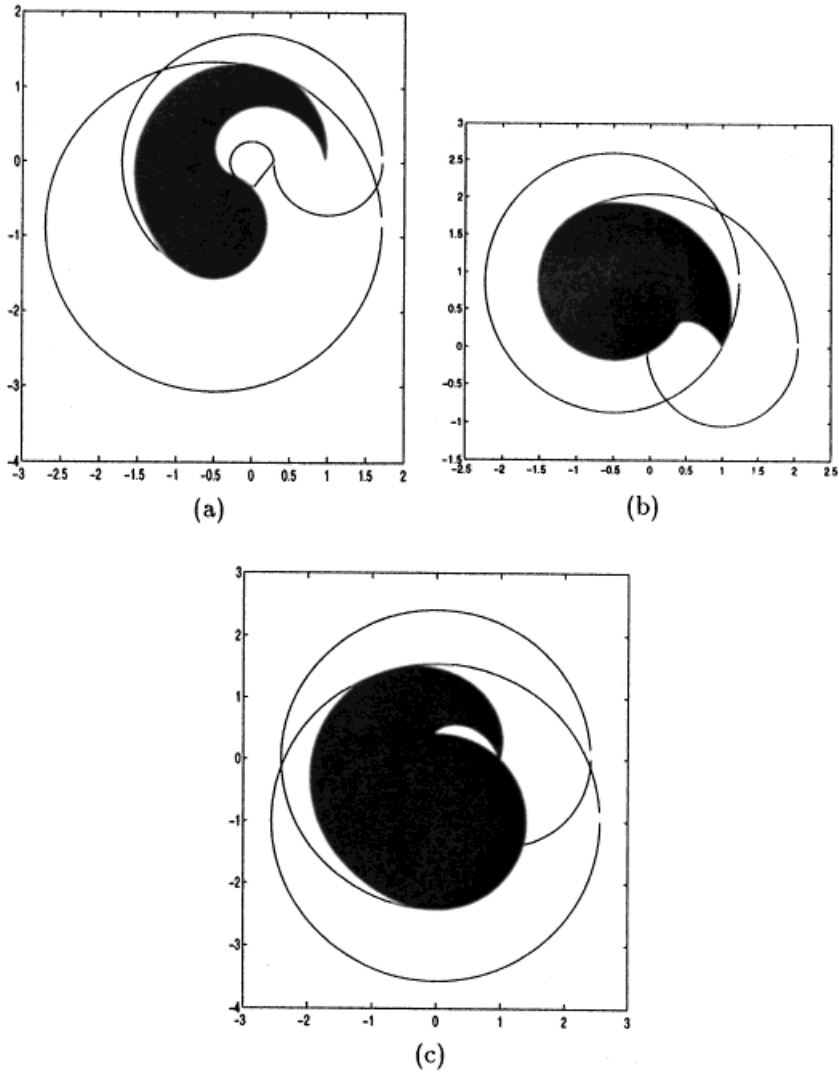


Fig. 13. Using the intersection of the two approximations to get a better superset. The same  $v$  and  $\omega$  as in Fig. 4(a)–(c).

**7. On disc-shaped objects and the effect of time delay**

*Disc-shaped objects.* It has been assumed until now that the obstacle  $O$  and robot  $R$  are two points in the plane. Now, let  $O$  and  $R$  be two discs, of the radii  $r_O$  and  $r_R$ , respectively. The locations of the discs’ centres will be referred to as the discs’ *positions*. For this case, denote the Hazard Region as  $HRS(C, v, r_O, r_R)$ ; as before,  $C$  is the robot’s path, and  $v$  the obstacle’s velocity (the robot’s velocity is  $v_R = 1$ ). The following proposition evaluates the effect of dimensional objects on HR (see Fig. 14):

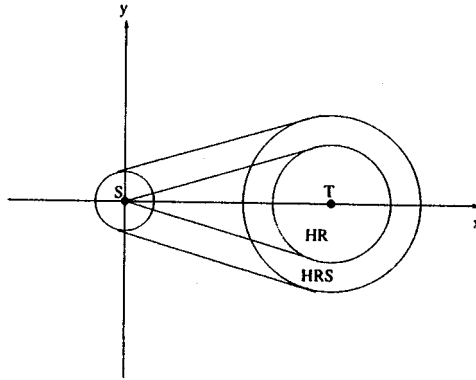


Fig. 14. For the straight-line motion, the enlarged Hazard Region HRs appears in two cases: (1) when the obstacle  $O$  or/and robot  $R$  are discs; (2) when there is a time delay between  $O$  and  $R$  starting moments.

**Proposition 15.** *If the obstacle  $O$  and robot  $R$  are two discs, of the radii  $r_O$  and  $r_R$ , respectively, then:*

$$\text{HRS}(C, v, r_O, r_R) = \{P \mid \exists Q \in \text{HR}(C, v) \text{ such that } |PQ| \leq r_O + r_R\}. \tag{22}$$

To see this, consider the hazard disc HD where  $R$  is at point  $M$  of its path  $C$ , Fig. 1. When  $O$  and  $R$  being two points, the radius of HD is  $vt_M$ . Now, with  $O$  and  $R$  becoming two discs, in order for  $R$  not to be captured by  $O$  at point  $M$ , the distance between the centres of  $R$  and  $O$  must be at least  $r_O + r_R$ . This means that the HD is enlarged to the radius  $vt_M + r_O + r_R$ . By Proposition 3, the HR itself is also enlarged (see Proposition 15).

*Effect of time delay.* A seemingly different but procedurally identical problem is the effect of time delay. Suppose obstacle  $O$  starts at time  $t = 0$ , while  $R$  starts at time  $t' \neq 0$ . Denote the modified HR as  $\text{HR}_{t'}(C, v)$ . Again, consider the hazard disc HD at point  $M$ , Fig. 1. Instead of radius  $vt_M$  (as in the case when  $O$  and  $R$  are points), now its radius will be  $vt_M + vt'$ , because when  $R$  reaches point  $M$ ,  $O$  has already been moving for time  $t_M + t'$ . The result is very similar to that for disc-shaped  $O$  and  $R$  above:

**Proposition 16.**  $\text{HR}_{t'}(C, v) = \{P \mid \exists Q \in \text{HR}_0(C, v), \text{ such that } |PQ| \leq vt'\}.$

The effect of time delay on HR is more complex when path  $C$  is a curve rather than a straight line. Namely, when  $C$  presents a number of primitives  $C_i$  connected together, HR will be the union of HRs for  $C_i$ , and all of them, except the first one,  $\text{HR}(C_0, v)$ , are affected by the time delay:

**Proposition 17.** *Suppose  $C = C_0 \cup C_1 \cup \dots \cup C_m$ , and the length of  $C_i$  is  $d_i$ ; then:*

$$\text{HR}(C, v) = \bigcup_{i=1}^m \text{HR}_{t_i}(C_i, v)$$

where  $t' = 0$  and  $t_i = \sum_{j=1}^{i-1} d_j$  (for  $i = 1, 2, \dots, m$ ).

This proposition will be the basis of our application of hazard region analysis to the case of optimal path with constrained curvature considered in the next section. Still remained to be considered here is the effect of the time delay on our two approximate solutions. According to the definitions and both solutions, the boundary of each solution is a union of circular arcs. This makes it easy to find the HR with time delay—it is just a set of points within certain distance to the original HR (without time delay), and its boundary is still a union of circular arcs (which can be easily obtained).

**8. Hazard region for a complex multi-segment path**

The following theorem sums up the results of HR analysis for a simple (straight line or circular arc) path  $C$ :

**Theorem 1.** *Let  $S$  and  $T$  be the two endpoints of path  $C$ .*

1. *If  $v \geq 1$  and the length of  $C$  is  $d$ , then  $HR(C, v) = \{P_0 \mid |P_0T| \leq vd\}$ .*
2. *If  $v < 1$  and  $C$  is a straight-line segment, then*

$$HR(C, v) = \{P_0 \mid |P_0T| \leq vd, \text{ or } |P_0T| \leq d, \text{ or } |P_0, ST| \leq 1/u |P_0S|\}, \text{ where } u = \sqrt{1 - v^2}.$$

3. *Let  $A_1 = \{P_0 \mid |P_0T| \leq D\}$  and  $A_2 = \{P_0 \mid |P_0T| \leq v\omega \text{ or } |P_0S| \leq v\omega \text{ or } |P_0O| \in [1 - v\omega, 1 + \omega] \text{ and the angle } P_0OS \in [0, \omega]\}$ , where*

$$D = \begin{cases} 2 \sin \omega/2 & \text{(if } \omega < 2 \cos^{-1} v) \\ 2u + v(\omega - 2 \cos^{-1} v) & \text{(if } \omega \geq 2 \cos^{-1} v) \end{cases}$$

*Then, if  $v > 1$  and  $C$  is an arc of  $\omega$  radians, with center  $O$  and radius 1, the hazard region  $HR(C, v)$  is contained in  $A_1 \cap A_2$ .*

Suppose now that the path  $C$  consists of a few sequentially connected primitives; each primitive is a straight line segment or a circular arc. Then the procedure for finding the corresponding HR is as follows:

1. Find the corresponding parameters of every path segment.
2. Find the HR without time delay for each path segment using the theorem above.
3. Find the time delay for each path segment; then, using Proposition 17 in the last section, find the corresponding HRs that take into account the time delays.
4. Find the entire HR, which is the union of the HRs found in step 3.

**9. Example: hazard region for the optimal path with constrained curvature**

To demonstrate the use of the developed methodology for computing hazard regions, consider now a more realistic situation when the robot’s motion is subject to kinematic constraints (a non-holonomic system). One such typical constraint is a limit

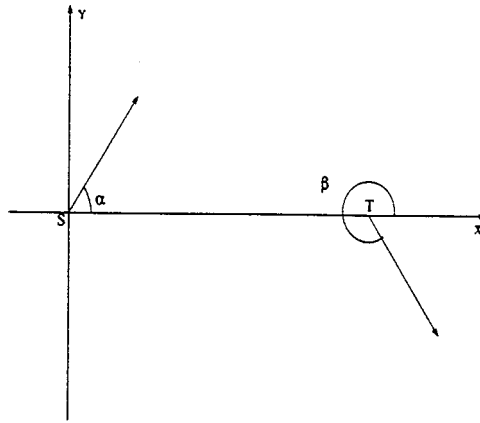


Fig. 15. The initial and final orientation angles,  $\alpha$  and  $\beta$ .

on the turning angle (as in an automobile). Suppose a car starts at some point  $S$  with the orientation  $\alpha$ , Fig. 15, and eventually arrives at point  $T$  with the orientation  $\beta$ . The car can move only along smooth paths that consist of combinations of straight-line segments and circular arcs of radius not less than  $r$ .

It has been shown by L. Dubins in 1957 [1] that in this case the optimal (i.e. the shortest, or geodesic) path consists of exactly three path segments and presents a sequence CCC or CSC, where  $C$  (for “circle”) is an arc of the maximal curvature  $1/r$ , and  $S$  (for “straight”) is a straight-line segment. As each arc  $C$  has two options for turning—right or left—the many combinations of paths that appear can be reduced to the *Dubins set* which includes six paths. The latter can then be computed and compared explicitly, to arrive at the optimal path. It has been further shown [11] that in the common case when the distance between points  $S$  and  $T$  is sufficiently large, the pair of orientations  $(\alpha, \beta)$  can be analyzed via a simple logical scheme, to arrive at the optimal path directly, without an exhaustive computation of the Dubins set. This means the computation of optimal paths for such non-holonomic systems can be done very fast and can be used for real-time motion planning. Figure 16 shows two examples of the optimal paths.

To find the hazard region HR for this kind of paths, first the HR for each of the path segments is found, in a standard coordinate system as presented above. Then the corresponding time delays are incorporated, producing the modified HRs. Finally, after the latter are translated into the current co-ordinate system, Proposition 17 is used to form the HR for the whole path.

To accomplish this sequence, a number of parameters of the path primitives are needed—the lengths of the straight line and two circular arc segments, along with their position parameters. All those are shown in Fig. 17.

Given:

$\alpha$ : initial orientation angle

$\beta$ : final orientation angle

$d$ : distance between points  $S$  and  $T$

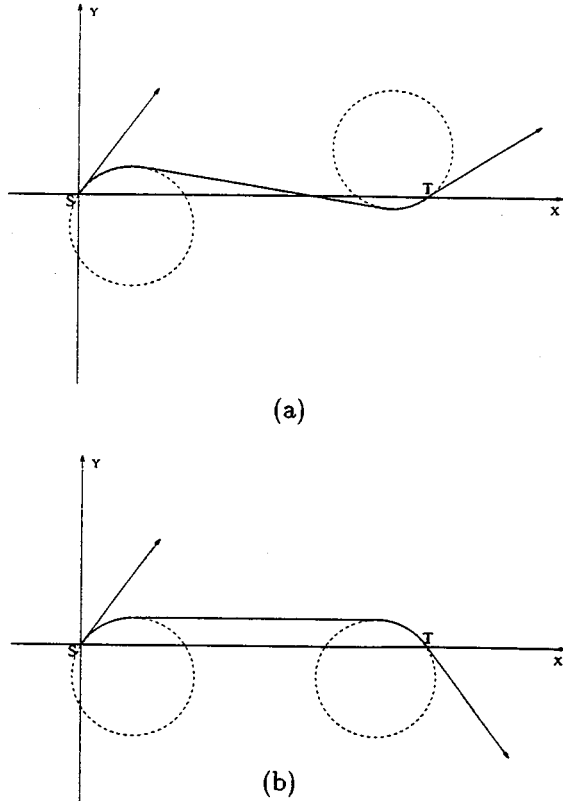


Fig. 16. Two examples of optimal paths between starting and target points  $S$  and  $T$ . Orientations at  $S$  and  $T$  are indicated by arrows. Each path consists of two circular arcs plus a straight-line segment in between.

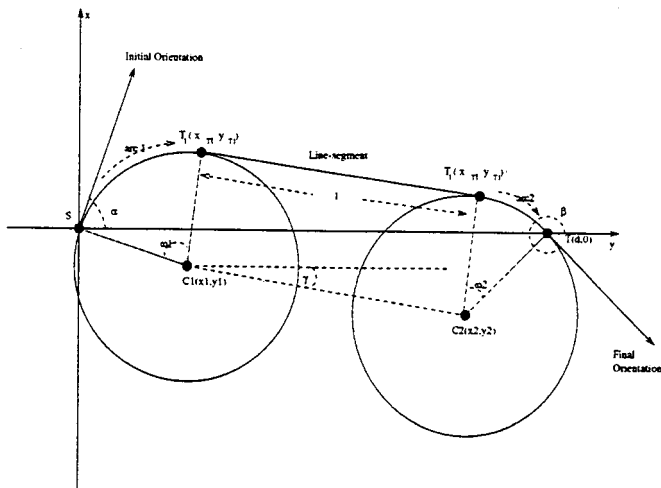


Fig. 17. The co-ordinate system.

Path segment parameters:

- $(x_{T_1}, y_{T_1})$ : co-ordinates of  $T_1$ , the endpoint of the first path segment
- $(x_{T_2}, y_{T_2})$ : co-ordinates of  $T_2$ , the endpoint of the second path segment
- $l$ : the length of the second (straight line) path segment
- $\omega_1$ : the length of the first (circular) path segment
- $\omega_2$ : the length of the third (circular) path segment
- $(x_1, y_1)$ : co-ordinates of  $C_1$ , the center of the first circular arc segment
- $(x_2, y_2)$ : co-ordinates of  $C_2$ , the center of the second circular arc
- $\gamma$ : the angle from positive  $x$ -axis to the line  $C_1C_2$ .

Then (see Fig. 17):

$$x_1 = \sin \alpha; \quad y_1 = -\cos \alpha; \quad x_2 = d + \sin \beta; \quad y_2 = -\cos \beta;$$

$$\gamma = \tan^{-1} \frac{\cos \alpha - \cos \beta}{d + \sin \beta - \sin \alpha}; \quad l = \sqrt{(d + \sin \beta - \sin \alpha)^2 + (\cos \beta - \cos \alpha)^2};$$

$$\omega_1 = \alpha - \gamma; \quad \omega_2 = 2\pi - \beta + \gamma;$$

$$x_{T_1} = \sin \alpha - \frac{\cos \alpha - \cos \beta}{l}; \quad y_{T_1} = \cos \alpha - \frac{d + \sin \beta - \sin \alpha}{l};$$

$$x_{T_2} = d + \sin \beta - \frac{\cos \alpha - \cos \beta}{l}; \quad y_{T_2} = -\cos \beta + \frac{d + \sin \beta - \sin \alpha}{l}.$$

The resulting hazard region is shown in Fig. 18.

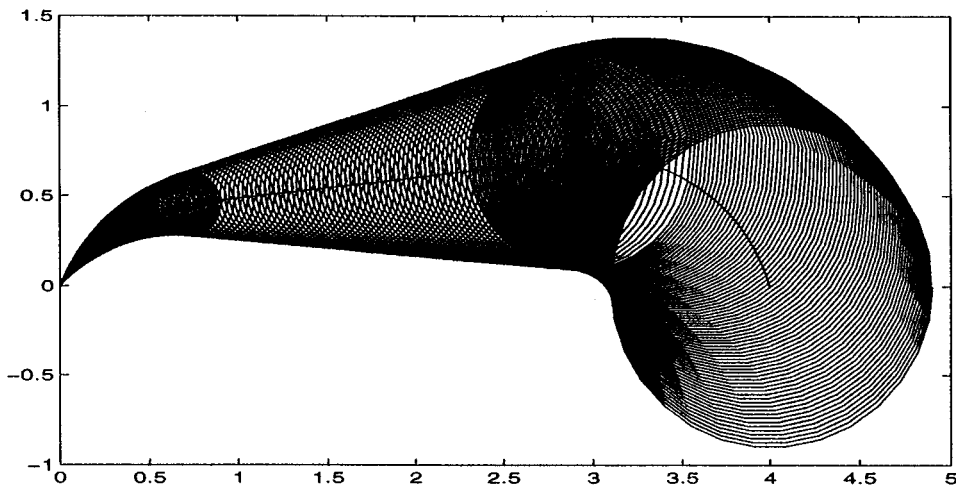


Fig. 18. The Hazard Region for the path in the example section 9;  $(0, 0)$  is the starting point.



## 10. Conclusion

The concept of hazard and safety regions, HR and SR, finds its applications in the general problem of motion planning, such as in pursuit games or in robot collision avoidance in an environment with moving objects. Presented here are two solutions to this problem: a precise solution for HR in the case of straight line motion, and an approximation solution for circular motion. The latter is obtained in three versions, with the third one being an intersection of the (basic) first two. The approximate solution works well for all possible cases, guarantees the safety of the robot, and is quite fast to obtain, thus allowing real-time implementation.

Besides classifying the areas in the plane as to their belonging to the hazard or safe regions, the results presented can also be used for designing more advanced motion planning algorithms, such as for continuously altering the contemplated path if a certain part of it is found to belong to the Hazard Region.

## References

1. Cameron, S. A., 'A study of the clash detection problem in robotics', *Proc. IEEE Int. Conf. on Robotics and Automation*, May 1985.
2. Canny, J., 'Collision detection for moving polyhedra', *IEEE Trans. Pattern Anal. Mach. Intelligence*, **5** (1986).
3. Dubins, L. E., 'On curves of minimal length with a constraint on average curvature, and with prescribed initial and terminal positions and tangents', *American J. Math.*, **79**, 497–516 (1957).
4. Fujimura, K., *Motion Planning in Dynamic Environments*, Springer, New York, 1991.
5. Fujimura, K. and Samet, H., 'An intersection algorithm for moving parts', *Proc. NASA Symp. on Computer Aided Geometry Modeling*, May 1983, Hapton, VA.
6. Lin, M. and Canny, J., 'A fast algorithm for incremental distance calculation', *Proc. IEEE Int. Conf. on Robotics and Automation*, May 1991, Sacramento, CA.
7. Liu, Y., Naborio, H. and Arimoto, S., 'A new solid model HSM for checking on interference between moving robots'. *J. Robotics Soc. Japan*, **7** (1989).
8. Lumelsky, V., Shen, L. and Shkel, A., 'Hazard and safety regions for paths with constrained curvature', *Technical Report RL-97001*, Robotics Laboratory, University of Wisconsin-Madison, February 1997.
9. Ong, C. J. and Gilbert, E., 'Growth distances: new measures for object separation and penetration', *IEEE J. Robotics Autom.* **12** (1996).
10. Ottman, T. and Wood, D., 'Dynamic sets of points', *Computer Vision, Graphics, and Image Processing*, **27** (1984).
11. Shkel, A. and Lumelsky, V., 'On calculation of optimal paths with constrained curvature: The case of long paths', *Proc. IEEE Intern. Conf. on Robotics and Automation*, May 1996, Minneapolis, MN.